

# Propagation of Shock Waves in Type-II Presupernovae

A. Yu. Deputovich and D. K. Nadyozhin

*Institute of Theoretical and Experimental Physics, ul. Bol'shaya Cheredushkinskaya 25, Moscow, 117259 Russia*

Received April 6, 1999

**Abstract**—We explore the reliability of the approximate methods which are used to estimate the velocity and temperature at the front of a shock wave that passes in a type-II presupernova successively through the carbon-oxygen shell, the helium shell, and the base of the hydrogen-helium envelope. This issue deserves a special consideration, because the attendant nucleosynthesis depends on the shock-front temperature and on other hydrodynamic parameters. The temperature of the shock-heated matter in the carbon-oxygen and silicon shells is shown to be so high that the contribution of electron-positron pairs to the equation of state becomes appreciable.

## INTRODUCTION

A detailed modeling and analysis of the observations of type-II supernovae (SNe II), as well as type-Ib and Ic supernovae, show that the main cause (trigger) of the explosion is gravitational collapse of the iron stellar cores into a neutron star (or even a black hole). As a result, the star breaks up into two parts: an expanding envelope and a collapsing core. An energy of  $\sim(1-2) \times 10^{51}$  erg is transferred to the envelope. This energy accounts for only a small fraction of the energy released during the collapse ( $\sim 3 \times 10^{53}$  erg), which is carried away largely in the form of neutrinos. Although the particular features of the mechanism that rips the star in two parts is not clear so far, the theory of SNe II continues to develop rapidly. The point is that the great differences in energetics and time scales (seconds for the collapse and days for the ejected envelope) allow the theoretical description of a SN II explosion to be separated into internal and external problems (see, e.g., Imshennik and Nadyozhin 1988). The presence of an envelope has virtually no effect on the dynamics of gravitational collapse and the neutrino-flux characteristics, while the envelope ejection and the supernova radiation do not depend on how the energy is transferred to the envelope (the only factor that matters is that this process occurs in a short time). The energy which is transferred to the envelope (below called the SN explosion energy) plays the role of a coupling parameter between the internal problem and the external problem. The interface between the collapsing core and the envelope lies somewhere near the outer boundary of the stellar iron core. The explosion energy is transferred to the envelope by a shock wave (SW) which passes gradually through chemically different shells: the silicon, carbon-oxygen, and helium shells and, finally, the outer shell with essentially initial hydrogen and helium abundances.

Considerable progress that has been made in recent years in the theory of nucleosynthesis in SN II envelopes (Woosley and Weaver 1995; Thielemann *et al.*

1996) allows not only such conventional means as a comparison of the observed and theoretical light curves and spectra, but also the isotopic composition of the ejected matter to be used to refine supernova models. Nucleosynthesis calculation is a complex problem per se, which can be solved in principle by combining the hydrodynamic code for computing SN explosions and the nucleosynthesis code into a single “supercode”. However, it is appropriate (and methodically more reliable) to separate the nucleosynthesis calculation from the hydrodynamic supernova calculation, using the temperature and density in the first calculation and, for neutrino nucleosynthesis, also the radii of the various stellar shells which are obtained from the hydrodynamic code.

In this paper, we explore the reliability of the approximate methods which are used in the literature to describe the parameters of shock waves as they pass through chemically different shells—the methods of Weaver and Woosley (1980) (WW) and Klimishin and Gnatyk (1981) (KG). We focus our attention on the carbon-oxygen and helium shells, where the details of the SN explosion mechanism definitely do not matter, which cannot be completely guaranteed for the silicon shell adjacent to the iron core.

## FORMULATION OF THE PROBLEM

In order to estimate the accuracy of the approximate methods, we computed a spherically symmetric hydrodynamic model of SN explosion by means of the SNV code, which has long been used at the Institute of Theoretical and Experimental Physics (see, e.g., Litvinova and Nadyozhin 1983). Since radiative heat conduction can be disregarded in this problem, the SNV code was used in its simplest mode—the equations of adiabatic hydrodynamics were numerically computed by using an explicit difference scheme. The shock waves were described by the method of fictitious viscosity.

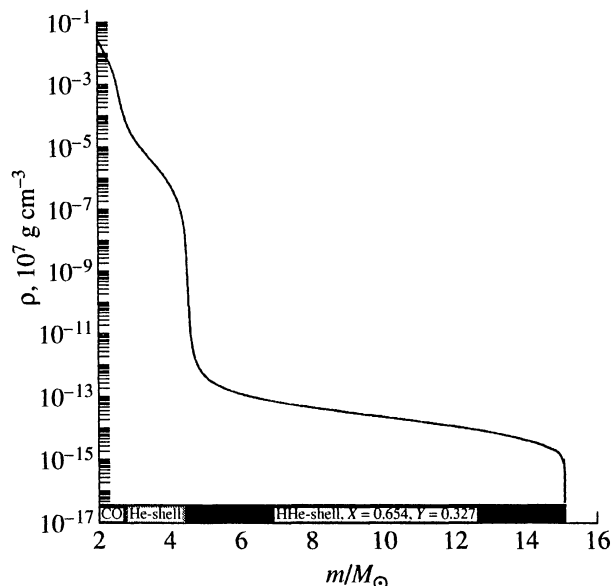


Fig. 1. Initial density distribution along the stellar radius.

As the initial model, we took the evolutionary model of a  $15.08M_{\odot}$  presupernova with initial solar chemical composition, which can be considered as a typical representative of the type-II presupernovae, computed by Woosley and Weaver (1995). The model represents a red supergiant ( $R = 490R_{\odot}$ ,  $T_{\text{eff}} = 4500$  K) with a  $1.41M_{\odot}$  iron core surrounded by chemically different shells. A simplified shell structure of the model which is adequate for our purposes is given in Table 1, and the density distribution in the outer part of the model under study ( $m \geq 2M_{\odot}$ ) is shown in Fig. 1. The abrupt decrease in density at the boundary between the carbon-oxygen and helium shells and, in particular, between the helium shell and the hydrogen-helium envelope is a crucial factor for the entire hydrodynamic process of SW passage through the presupernova.

Since we are primarily interested in the carbon-oxygen and helium shells, we placed the inner boundary at  $m = 1.55M_{\odot}$  (near the outer boundary of the silicon shell), i.e., we performed the calculations by using the hydrodynamic code for the outer part of the presupernova ( $1.55M_{\odot} < m < 15.08M_{\odot}$ ), which is known to be ejected into the interstellar medium during the supernova explosion. The explosion itself was simulated by an instantaneous energy release in the shell  $\Delta m = 0.1M_{\odot}$  ( $1.55M_{\odot} < m < 1.65M_{\odot}$ ) immediately adjacent

to the inner boundary. The explosion energy  $E_{\text{exp}} = 2.3 \times 10^{51}$  erg was released either by specifying an outward-directed initial velocity of the matter or by a corresponding increase in the temperature of the matter in this shell. As one might expect, the results of the calculations turned out to be completely insensitive to the way in which the energy is released.

In our calculations, we used the equation of state for a completely ionized matter with blackbody radiation; the electron-positron component was described by taking into account degeneracy and pair formation (Blinnikov *et al.* 1996).

According to the method by Weaver and Woosley (1980), the SW-front temperature  $T_{\text{SW}}$  is estimated by equating the explosion energy to the energy of blackbody radiation in the volume enclosed by the SW front (in a sphere of radius  $R_{\text{SW}}$ ):

$$E_{\text{exp}} = aT_{\text{SW}}^4 \times \frac{4}{3}\pi R_{\text{SW}}^3. \quad (1)$$

In this case, the entire explosion energy is implicitly assumed to be concentrated in the radiation energy and uniformly distributed inside this sphere, where the temperature is constant and equal to  $T_{\text{SW}}$ .

The approximate method by Klimishin and Gnatyk (1981) allows the SW-front velocity  $D$  to be estimated from the local preshock density  $\rho_1(R_{\text{SW}})$ :

$$D = \begin{cases} C_d(\rho_1 R_{\text{SW}}^3)^{-1/2} & \text{for decelerating SW,} \\ C_a(\rho_1 R_{\text{SW}}^3)^{-1/5} & \text{for an accelerating SW,} \end{cases} \quad (2)$$

where  $C_d$  and  $C_a$  are constants which are chosen in each specific problem. If  $D$  is known, the SW-front temperature can be determined from Hugoniot's conditions. When the preshock velocity of the matter can be ignored (our case), Hugoniot's conditions are

$$\rho_2(D - u_2) = \rho_1 D, \quad (3)$$

$$P_2 + \rho_2(D - u_2)^2 = P_1 + \rho_1 D^2, \quad (4)$$

$$W_2 + \frac{1}{2}(D - u_2)^2 = W_1 + \frac{1}{2}D^2, \quad (5)$$

where  $P$ ,  $W$ , and  $u$  are the pressure, enthalpy, and velocity of the matter. The subscripts 1 and 2 refer to the pre- and postshock quantities, respectively.

Given the preshock density  $\rho_1$ , the equation of state  $P = P(T, \rho)$ ,  $W = W(T, \rho)$ , and the velocity  $D$  (2), the temperature  $T_{\text{SW}} \equiv T_2$  in the KG method is determined

Table 1. Shell structure of the initial model

Mass, $m/M_{\odot}$	1.41–1.61	1.61–2.69	2.69–4.45	4.45–15.08
Radius, $r/10^8$ cm	1.47–2.25	2.25–30.8	30.8–550	$550-3.4 \times 10^5$
Chemical composition	Si	O, C	He	He, H
Mass fraction	1	0.5, 0.5	1	0.33, 0.65

1999ASSTL...25...649D

by solving Eqs. (3)–(5) by iterations using the Newton method. The numerical value for one of the constants in Eq. (2) (in our case, for  $C_d$ , because the SW first decelerates) was chosen so that the velocity  $D$  from (2) matched its value obtained from the hydrodynamic calculation immediately after the SW formation. Subsequently, when the SW-front acceleration changes sign, the constants  $C_d$  and  $C_a$  replace each other in such a way that the front velocity  $D$  remains continuous. Note that the change of sign of the SW acceleration in (2) matches the change of sign of the derivative  $d(\rho_1 R_{SW}^3)/dr$ .

RESULTS

The results of our calculations are presented in the form of distributions of physical quantities along the stellar radius and their values at the SW front. We kept track of the SW position in each step of the hydrodynamic calculation by locating the abrupt change in the velocity of the matter, which was usually smeared by fictitious viscosity over two or three zones. For this reason, to determine the SW-front position more accurately, we also located the abrupt change in fictitious viscosity, which is displaced from the abrupt change in velocity by no more than one zone. We then determined the refined SW-front position by interpolation. This combined approach allowed us to reduce considerably the numerical “noise” when computing the front velocity  $D$  by numerical differentiation:  $D = dR_{SW}/dt$ .

To check our results for reliability, we also changed the number of grid points in the model. We performed our calculations for 346 zones (the number of zones in Woosley-Weaver’s original model), as well as for 692 and 1384 zones. It turned out that increasing the number of zones caused the numerical noise to decrease only slightly and did not affect our results. The results in the figures refer to the calculations for 692 zones.

Figure 2 shows the SW-front temperature distributions that were obtained in the hydrodynamic calculation, as well as by using the KG and WW methods. The KG method is seen to describe well the behavior of the SW front at the initial stage of shock propagation in the carbon-oxygen and helium shells. However, as the SW

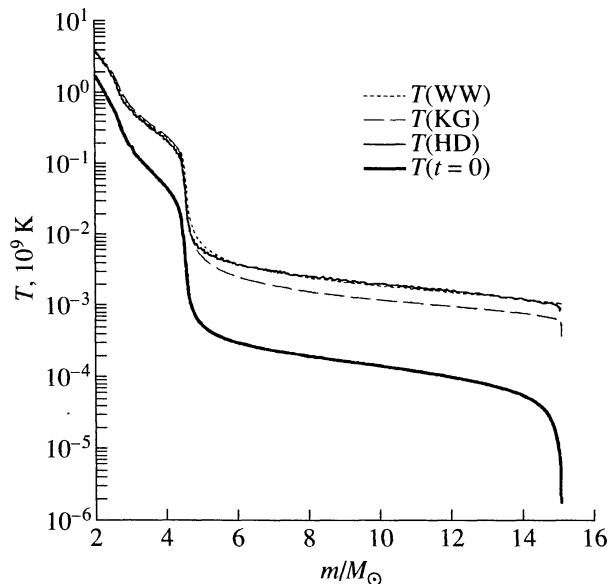


Fig. 2. Shock-front temperature versus  $m$ : the initial temperature distribution in the star  $T(t = 0)$  (heavy line); the SW-front temperature as determined by the hydrodynamic method,  $T(HD)$  (thin line); the front temperature computed by the WW method,  $T(WW)$  (short dashes); and the front temperature computed by the KG method,  $T(KG)$  (long dashes).

passes into the helium-hydrogen envelope, the SW-front temperature, according to this method, turns out to be approximately half its actual value. The probable reason is that, although formulas (2) describe well the shock waves which travel with a smoothly changing velocity, when the SW-front velocity changes abruptly in the region  $4.6\text{--}5.0M_{\odot}$  (the beginning of the hydrogen-helium envelope), the formulas of the KG method yield an underestimated value of  $C_d$  and, consequently, an underestimated SW velocity. Subsequently, when the velocity curve again becomes gently sloping, the formulas of the KG method again begin to describe correctly the processes at work, although the velocity curve of the KG method turns out to lie below the true curve because of the errors in the previous steps. This is evident from the fact that, if we move this segment of

Table 2. Relationship between the internal and kinetic energies of the presupernova envelope

Time from beginning of SW propagation, s	SW-front position, $M_{\odot}$	$E_{int}, 10^{50}$ erg	$E_{grav}, 10^{50}$ erg	$E_{kin}, 10^{50}$ erg
1.5	2.1	21.5	-9.38	7.30
25	4.1	8.16	-1.02	12.3
128	4.5	3.12	-0.28	16.6
514	4.72	1.86	-0.07	17.6
5190	5.72	4.77	-0.03	14.7
23200	9.85	8.97	-0.02	10.4
49400	13.8	9.83	-0.01	9.60

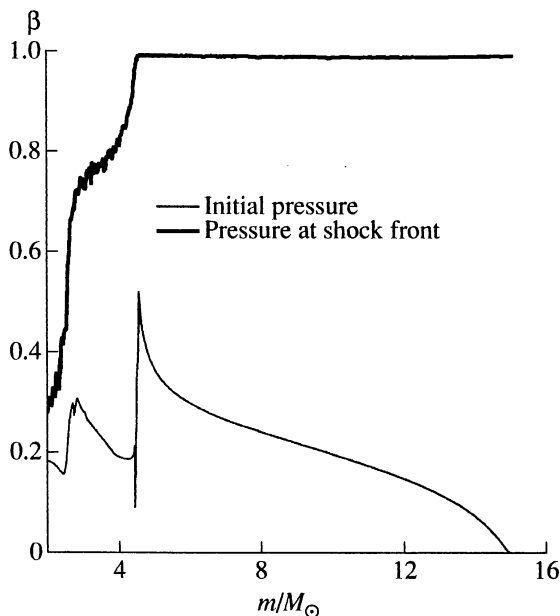


Fig. 3. Radiation-to-total pressure ratio  $\beta$  versus  $m$ :  $\beta(m)$  in the initial presupernova model before the explosion (thin line); and  $\beta$  at the SW front (heavy line).

the curve of the KG method upward starting from  $6M_{\odot}$ , then it will closely coincide with the curve that was constructed by using the hydrodynamic model. This result can also be explained by the fact that formulas (2) were derived and tested when studying the passage of shocks in supernova outer envelopes, where the density changes considerably more slowly than it does at the boundary between the helium shell and the hydrogen-helium envelope.

By contrast, the approximation of the WW method is generally in excellent agreement with our calculations, and only on either side of the boundary between the helium shell and the hydrogen-helium envelope does it yield a value which differs by  $\sim 20\%$  from that obtained in the hydrodynamic calculation; the width of the segments with a discrepancy does not exceed  $0.6M_{\odot}$ . At first glance, this result is rather strange. Indeed, let us take a look at Table 2, which gives the kinetic, thermal, and gravitational energies of the stellar envelope. We see from this table that the internal energy at the initial stages of SW propagation dominates over the kinetic energy. Subsequently, as the SW front enters the hydrogen-helium envelope, the kinetic energy exceeds the internal energy by almost an order of magnitude. Later, however, when the SW is located in the middle part of the hydrogen-helium envelope, the initial explosion energy is approximately evenly divided between the kinetic and internal energies.

The internal energy in a sphere of radius  $R_{\text{SW}}$  can be written as

$$E_{\text{int}} = a \langle T \rangle^4 \times \frac{4}{3} \pi R_{\text{SW}}^3, \quad (6)$$

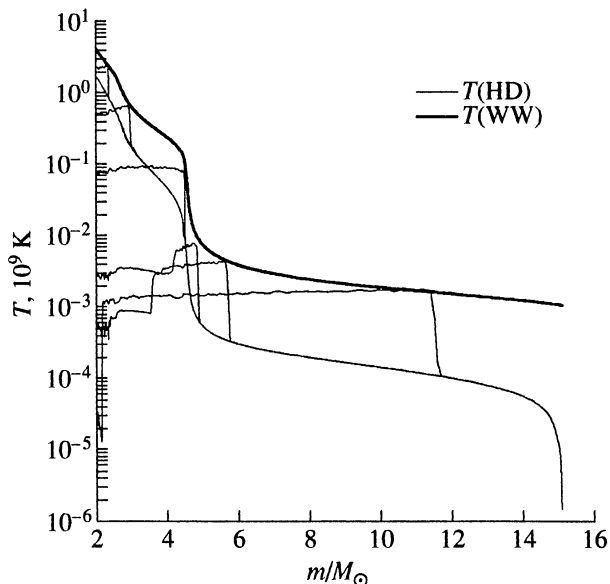


Fig. 4. Temperature distribution along the stellar radius. The thin lines represent the temperature distributions along the stellar radius at various times ( $t = 1, 3, 58, 1345, 4921,$  and  $30900$  s); the heavy line represents the SW-front temperature computed by the WW method.

where  $E_{\text{int}}$  is the part of the explosion energy which transforms into the internal energy of the matter, and  $\langle T \rangle$  is the mean temperature in the region enclosed by the SW front which generally depends on  $R_{\text{SW}}$ . Equation (6) holds when blackbody radiation makes a major contribution to the equation of state. As we see from Fig. 3, this assumption is indeed a good approximation in our case. Formula (1) is derived by substituting  $E_{\text{int}}$  for  $E_{\text{exp}}$  and  $T_{\text{SW}}$  for  $\langle T \rangle$  in (6). If the temperature in the hydrodynamic calculation were constant everywhere behind the SW front (i.e., if  $\langle T \rangle$  were equal to  $T_{\text{SW}}$ ), then formula (1) would yield a factor of  $\sqrt[4]{E_{\text{exp}}/E_{\text{int}}}$  larger value of  $T_{\text{SW}}$ . According to Table 2, a factor of  $\sqrt[4]{2} \approx 1.2$  as a minimum and a factor of  $\sqrt[4]{9} \approx 1.8$  as a maximum. Since the postshock temperature actually decreases toward the stellar center (Fig. 4),  $\langle T \rangle$  is always lower than  $T_{\text{SW}}$ . Surprisingly, the substitution of  $E_{\text{exp}}$  for  $E_{\text{int}}$  in (1) is almost exactly offset by the substitution of  $T_{\text{SW}}$  for  $\langle T \rangle$ . In other words, with a high accuracy, the mean postshock temperature is related to the front temperature by

$$\langle T \rangle \approx T_{\text{SW}} \sqrt[4]{E_{\text{exp}}/E_{\text{int}}}. \quad (7)$$

This result is most likely a fortunate coincidence. This is indirectly confirmed by the fact that the formula

$$D = \sqrt{\frac{7 E_{\text{exp}}}{4 \pi \rho R^3}}, \quad (8)$$



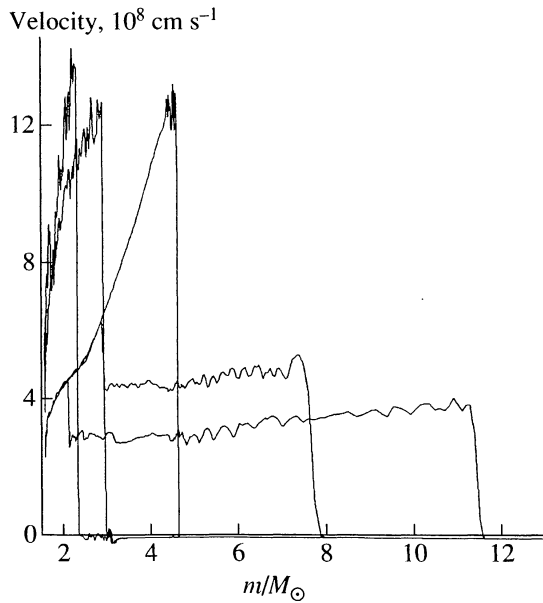


Fig. 5. Velocity distributions of the stellar matter at various times ( $t = 1, 3, 436, 13116, \text{ and } 30900 \text{ s}$ ).

which is derived by substituting  $P_2 = \frac{1}{3} a T_{\text{SW}}^4$  and  $\gamma = 4/3$  (a radiation-dominated SW) with  $T_{\text{SW}}$  from (1) in the expression for the pressure at the front of a strong SW,  $P_2 = \frac{2}{\gamma + 1} \rho_1 D^2$ , yields a greatly overestimated SW velocity. According to this formula, the shock velocity reaches  $70 \times 10^8 \text{ cm s}^{-1}$ .

Figure 5 shows velocity distributions for the matter at various times. These distributions reveal a large acceleration of the SW front and the postshock matter as the SW passes from the helium shell into the hydrogen-helium envelope, which accounts for such a high kinetic energy at this stage of SW propagation (see Table 2,  $t = 514 \text{ s}$ ). This acceleration produces a gas-dynamical impact on the outer hydrogen-helium envelope, which gives rise to a second reflected shock wave whose front travels inward through the matter and lies at  $m \approx 3$  and  $2M_{\odot}$  at  $t = 436$  and  $13116 \text{ s}$ , respectively. This front is seen in Fig. 4 as an abrupt change in temperature (see also Woosley and Weaver 1995).

Figure 6 shows the shock-front velocities that were determined by the KG method (heavy line) and in the hydrodynamic calculation (thin line). This plot is seen to be in close agreement with the plot for the temperature (Fig. 2). The velocities that were computed by the two methods match before the beginning of the hydrogen-helium envelope and then differ by a factor of 3 or 4.

Figure 7 shows the number of electron-positron pairs per “atomic” electron. We see from the plot that the number of pairs in the carbon-oxygen shell (and,

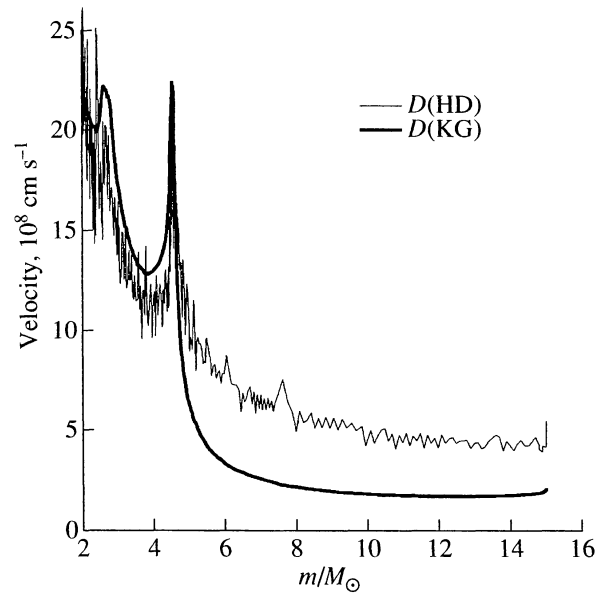


Fig. 6. SW-front velocity versus  $m$ : the front velocity computed with the hydrodynamic model,  $D(\text{HD})$  (thin line); and the front velocity computed by the KG method,  $D(\text{KG})$  (heavy line).

consequently, in the silicon shell) is comparable to the number of atomic electrons; this fact should be taken into account in the detailed calculations of nucleosynthesis in supernova envelopes. Note that when the number of pairs is equal to the number of atomic electrons, the total number of particles (electrons plus positrons) triples. In addition, the adiabatic index is smaller than  $4/3$ , and the limiting compression  $\rho_2/\rho_1$  can exceed 7 (Pinaeva 1964; Morozov 1983).

To check whether the laws of conservation of mass, momentum, and energy are correctly reproduced in the hydrodynamic calculations by the method of fictitious viscosity, we substituted  $P_2$ ,  $\rho_2$ ,  $u_2$ , and  $W_2$  from the hydrodynamic calculations into each of the equations (3)–(5) and computed three independent SW velocities, which must match. These values (dashed lines) and the SW velocity, which we computed by the method described at the beginning of this section, are shown in Fig. 8. Since the dashed line, which corresponds to the equation of conservation of mass (3), essentially coincides with  $D$  from the hydrodynamic calculation, it is virtually invisible. The values of  $D$  calculated from Eqs. (4) and (3) (the lower and upper dashed lines, respectively) differ slightly (within  $\sim 20\%$ ). Since the resolution of the difference scheme is one zone, such differences in  $D$  are natural when all three relations (3)–(5) are considered in the same zone, which is associated with the location of the SW-front.

Finally, Fig. 9 shows the specific entropy per nucleon. The high peak in the SW-acceleration region at the boundary between the helium shell and the

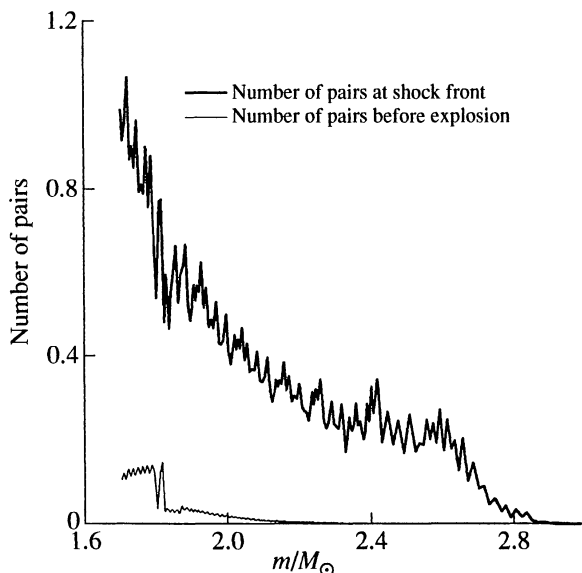


Fig. 7. Relative number of electron-positron pairs at the SW front versus  $m$ . The thin line represents the distribution of the number of pairs along the stellar radius before the explosion; and the heavy line represents the number of pairs at the shock front.

hydrogen-helium envelope,  $S \approx 1.1 \times 10^3 \frac{k}{m_u}$ , gives way

to an abrupt decrease in entropy with increasing  $m$ , creating favorable conditions in this region for the development of convective instability and Rayleigh-Taylor instability.

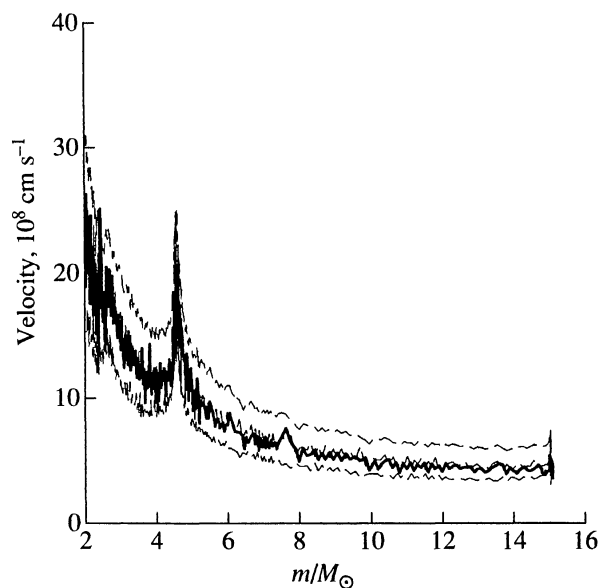


Fig. 8. Shock-front velocity calculated from Hugoniot's equations by substituting the physical parameters obtained in the hydrodynamic calculation into them (see text).

## CONCLUSION

Our main conclusions are as follows:

The approximate method of computing the SW-front temperature, which was proposed by Weaver and Woosley (1980), describes accurately the SW-front temperature  $T_{sw}$ . Small errors (no larger than 20%) near the helium-shell boundary are unlikely to reduce the value of this simple method. The method of estimating the SW-front velocity  $D$  proposed by Klimishin and Gnatyk (1981) in combination with Hugoniot's conditions for a strong shock wave is as good as Weaver-Woosley's method for computing  $T_{sw}$  in the carbon-oxygen and helium shells. It also yields a good estimate of  $D$  in these shells, while Weaver-Woosley's method gives greatly overestimated values. However, the velocity  $D$  in the hydrogen-helium envelope computed by Klimishin-Gnatyk's method is a factor of 3 or 4 and the corresponding temperature is a factor of  $\approx 2$  lower than the values obtained in hydrodynamic calculations.

In the silicon and carbon-oxygen shells, where the SW-front temperature reaches  $\sim (1-2) \times 10^9$  K, electron-positron pairs contribute appreciably to the equation of state. This contribution must be taken into account during detailed calculations of SW propagation in presupernovae.

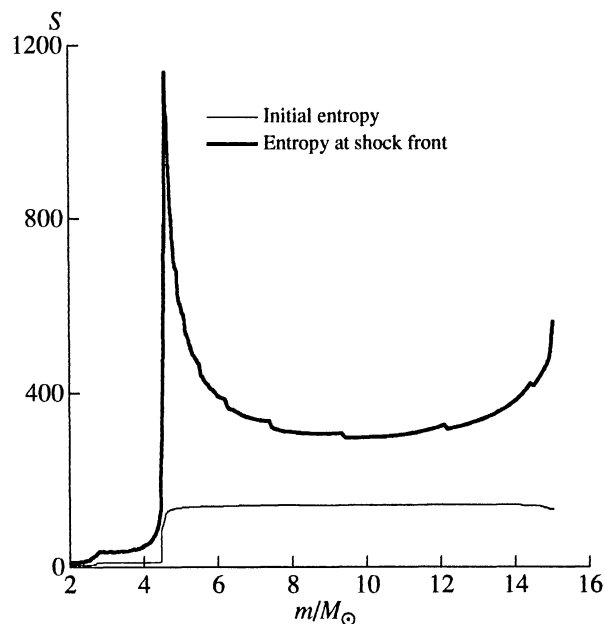


Fig. 9. Specific entropy per nucleon  $S \frac{m_u}{k}$  ( $k$  is the Boltzmann constant, and  $m_u$  is the atomic mass unit): the specific entropy along the stellar radius before the explosion (thin line); and the specific entropy at the shock front (heavy line).

## ACKNOWLEDGMENTS

We wish to thank S.E. Woosley and T.A. Weaver for providing the evolutionary model of a type-II presupernova. This study was supported by the International Science and Technology Center (project no. 370-97) and the Russian Foundation for Basic Research (project no. 96-15-96465).

## REFERENCES

- Blinnikov, S.I., Dunina-Barkovskaya, N.V., and Nadyozhin, D.K., *Astrophys. J., Suppl. Ser.*, 1996, vol. 106, p. 171.
- Imshennik, V.S. and Nadyozhin, D.K., *Usp. Fiz. Nauk*, 1988, vol. 156, p. 561.
- Klimishin, I.A. and Gnatyk, B.I., *Astrophysics*, 1981, vol. 17, p. 306.
- Litvinova, I.Yu. and Nadyozhin, D.K., *Astrophys. Space Sci.*, 1983, vol. 89, p. 89.
- Morozov, Yu.I., *Prepr. Inst. Teor. Eksp. Fiz.*, Moscow, 1983, no. 176.
- Pinaeva, T.V., *Astron. Zh.*, 1964, vol. 41, p. 25.
- Thielemann, F.-K., Nomoto, K., and Hashimoto, V., *Astrophys. J.*, 1996, vol. 460, p. 408.
- Weaver, T.A. and Woosley, S.E., *Ann. NY Acad. Sci.*, 1980, vol. 336, p. 335.
- Woosley, S.E. and Weaver, T.A., *Astrophys. J., Suppl. Ser.*, 1995, vol. 101, p. 181.

*Translated by V. Astakhov*